Available online at www.sciencedirect.com

ScienceDirect

Energy Procedia 81 (2015) 1131 – 1142

Energy Procedia

69th Conference of the Italian Thermal Machines Engineering Association, ATI2014

Numerical study of a micro gas turbine fed by liquid fuels: potentialities and critical issues

Raffaela Calabria[a], Fabio Chiariello[a], Patrizio Massoli[a], Fabrizio Reale[a]*

"Istituto Motori- CNR, via Marconi n.4, 80125, Naples, Italy"

Abstract

Aim of the paper is to evaluate the potentialities and critical issues of the micro-gas turbine Turbec T100 properly modified in order to be powered by liquid fuels. The main difference with respect to the version designed for gaseous fuels concerns the combustor, namely the combustion chamber and the fuel injection system. The numerical study was carried out using both a 0D matching analysis and a 3D CFD analysis of the combustor. The thermodynamic model, coupled with the operating maps of rotating components, was calibrated using the experimental data collected during operation of the micro-gas turbine with gaseous fuel. The operative parameters computed through the 0D model have been utilized to simulate the behavior of micro-gas turbine fed by liquid fuels, thus obtaining the initial and boundary conditions to be used in the CFD analysis. The combustion process of liquid fuels is analyzed; the main differences at varying loads are discussed in terms of temperature and velocity profiles of the air flows inside the combustion chamber and mean values of turbine inlet temperature and exhaust gaseous concentration. A preliminary study concerning the characteristics of the injection system is also reported.

Peer-review under responsibility of the Scientific Committee of ATI 2014

"Keywords: CFD analysis; micro gas turbine; combustion;"

* Corresponding author. Tel.: +39 0817177110 ; fax: +39 0812396097.
E-mail address: f.reale@im.cnr.it

Peer-review under responsibility of the Scientific Committee of ATI 2014
doi:10.1016/j.egypro.2015.12.138

1. Introduction

Micro gas turbines (MGT) represent one of most prone conversion systems for the realization of the distributed energy generation grids. This concurs with the European strategy for the build-up of a single, stronger and smarter electricity grid able to accommodate the massive deployment of renewable and decentralized energy sources [1].

The relevance in using MGT is related to both the possibility of using a wide range of fuels and the realization of efficient cogenerative cycles by recovering heat from the exhaust gases at higher temperatures. In this context, the studies on micro gas turbines are focused on the analysis of the machine versatility and flexibility, when operating conditions and fuels are significantly varied. Part load operations become central in order to obtain flexible energy systems that would be able to follow both final user requests and variations in renewable energy supply.

MGTs are attractive since they can utilize gaseous or liquid mineral fuels, biofuels or fuels of "opportunity". However, the variety of the energy sources and the corresponding large variation in fuel properties that can be expected, places relevant scientific and technological issues which need to be addressed [2, 3].

In recent years, the authors finalised both experimental and numerical studies to analyse the versatility of a micro gas turbine Turbec T100 fuelled with gaseous fuels, varying fuel and load [4-7]. Aim of the present paper is to explore the versatility of the micro-gas turbine Turbec T100 with the combustor designed for liquid fuels. To this purpose, the analysis of the comprehensive behavior of the machine as well as of the most significant components, namely the fuel injection systems and combustion chamber, is required. In particular, it is compared the behaviour of the combustors designed for gaseous and liquid fuels by analysing any variation in the combustion chamber flow field. Then it is reported a preliminary study of the combustion process in case of adoption of standard atomization models, focusing on the effects related to type and position of the injectors.

Nomenclature

GF	Gaseous fuel
LF	Liquid fuel
MGT	Micro Gas Turbine
TIT	Turbine Inlet Temperature, K
TOT	Turbine Outlet Temperature, K

2. Turbec T100: combustor description and model details

2.1. The combustor geometries for gaseous and liquid fuels

In Figure 1 the geometries of the combustors designed by Turbec, for gaseous (left) and liquid (right) fuels, are described. In both cases the combustion chamber is a reverse flow tubular combustor, made up by the inner flame tube, in which the combustion evolves, and the liner.

Pre-heated air, by a primary surface recuperator, is admitted in the combustion chamber at temperatures higher than 850 K. From Figure 1 it can be noted the dilution holes, located at the beginning of the liner, and the annular duct, between outer and inner flame tube. The principal purpose of the dilution holes is the reduction of the average outlet temperature to acceptable values for the radial turbine.

Air enters the combustion chamber in counter flow respect to combustion gases, feeding the primary and the secondary swirlers. In the gaseous fuel layout (GF combustor), fuel is supplied in two different lines: the pilot line (diffusive flame) and the main line (premixed flame). In the liquid fuels design (LF combustor), the fuel is sprayed in the combustion chamber by means an injector located axially on the swirler plate. In both GF and LF designs a third swirler is placed in correspondence of fuel inlet (pilot line/ liquid fuel injector), but in GF case, the air comes from combustor inlet, while for the LF geometry the air comes directly from a bleed after compressor outlet, at a temperature much lower than that of the combustion air (about 490 K respect 870 K in nominal case). The choice of the computational domain has been mainly driven by the inlet boundary conditions. Even though the combustor shows a fairly axial symmetric shape, the full domain has been discretized in order to consider the asymmetric flow supplied by the upstream diffuser [4].

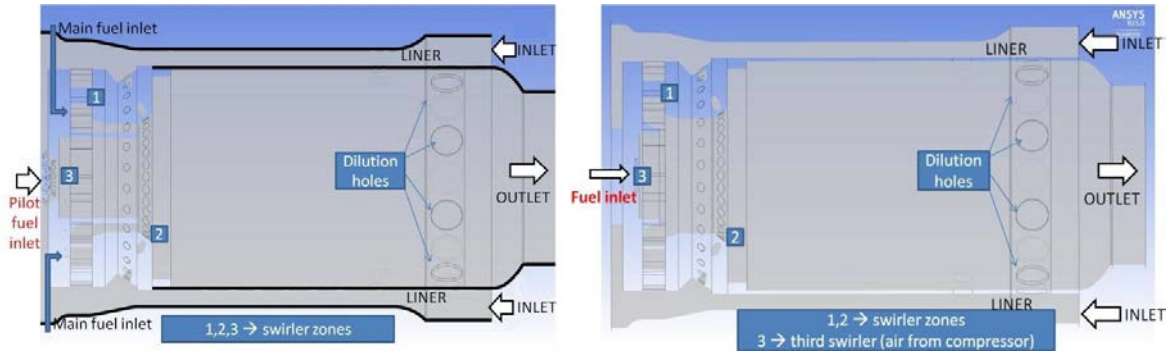

Fig. 1. Combustor scheme: GF (left) ; LF (right) .

In order to assure a complete structured grid, extensive use of non conformal interfaces has been adopted between swirlers and the chamber core. Parts of the internal walls have been explicitly meshed to include conjugate heat transfer, especially in the first section of the combustor where the incoming airflow from the compressor is further heated by the exhaust gases, effectively realizing an internal heat recovery. In both cases computational meshes were performed by ANSYS ICEM 13.0; the differences are shown in Table 1. Figure 2 shows a split view of the LF combustor mesh.

Table 1. Computational grid characteristics

	GF combustor	LF combustor
Type of mesh	Structured-multiblock	Structured-multiblock
Number of nodes	4.1 millions	3.7 millions
Minimum Orthogonal Quantity	0.327	0.25

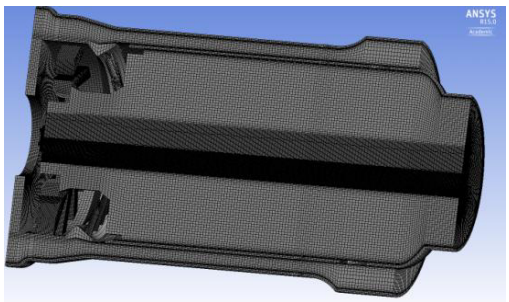

Fig. 2. 3D view of the computational domain

CFD analysis was performed by commercial code ANSYS CFX 15.0. The turbulence model was chosen after a sensibility analysis in order to highlight performances in terms of computational cost and thermodynamic parameters.

2.2. Turbulence modeling and flow fields comparison

A first phase of this study was focused on the analysis of air flow distributions by varying first turbulence models and then the type of combustor. For this analysis boundary conditions were taken from a previous authors' work [5] in operating conditions near the nominal one. In Table 2 boundary conditions are summarized:

Table 2. Combustor inlet boundary conditions - test case 1

Boundary conditions	Test case 1
Air mass flow, kg/s	0.785
Inlet Combustor Temperature, K	870
Inlet Combustor Pressure, bar	4,45

The turbulence models chosen for the sensibility analysis are all based on Reynolds Averaged Navier-Stokes (RANS) approach. In particular it was chosen to adopt a standard k - ε, a k- ω SST and a baseline Reynolds Stress Model (RSM) [8-13].

In order to analyze the differences between the results from the three models, the percentage distributions between dilution holes and swirlers have been calculated for the LF combustor (Table 3); Figure 3 shows the variations in terms of velocity magnitude. Subject of this analysis was the combustor modified in order to work with liquid fuels.

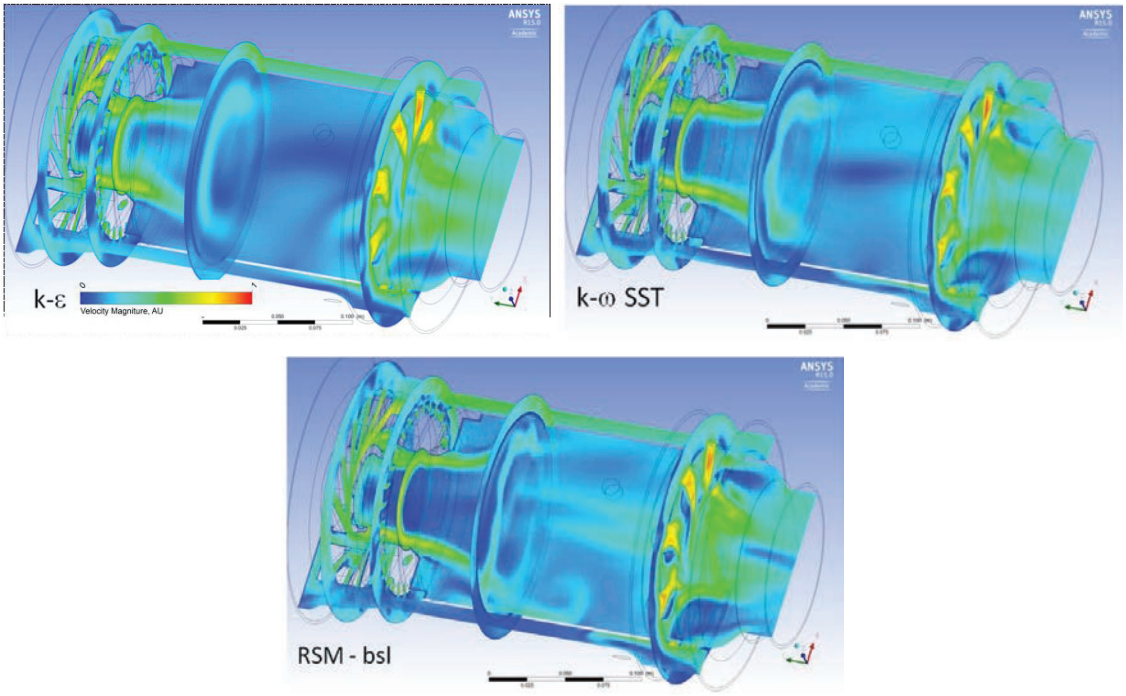

Fig. 3. Case model: LF Combustor. Velocity profiles in axial view and in four different cross sections, for different turbulence models

The flow distributions are similar and only the adoption of bsl RSM seems to show some differences in the velocity magnitude distributions. Thus, RSM model was chosen for the simulations of the combustion process in both GF and LF combustors according with literature [13], which recommends this model in case of strong swirled flows, such in this case.

Table 3. Case model: LF combustor. Flow distributions between holes and swirlers for the different turbulence models

RANS model	k - ε	k- ω SST	bsl RSM
Dilution holes	62.1%	62.1%	62.0%
First swirler	26.8%	26.7%	26.6%
Second swirler	10.9%	11.0%	11.3%
Third swirler	0.2%	0.2%	0.2%

It is worthwhile to underline that the percentage of air that comes to the third swirler is fixed and independent from turbulence models. In the LF combustor this air mass flow at lower temperature is used to confine the spray.

After choosing the turbulence model, the bsl RSM one, the focus was on the differences between LF and GF combustors in terms of flow distribution. The results are summarized in Table 4. As anticipated the main constructive difference in the design of GF and LF combustors regards the third swirler. In the GF scheme, the higher percentage of combustion air that comes at the third swirlers implies a lower rate in the first swirler.

Table 4. Flow distributions between holes and swirlers, in LF and GF combustors, computed by using bsl RSM turb. model

Combustor type	LF	GF
Dilution holes	62.0%	61.6%
First swirler	26.6%	24.5%
Second swirler	11.3%	11.4%
Third swirler	0.2%	2.4%

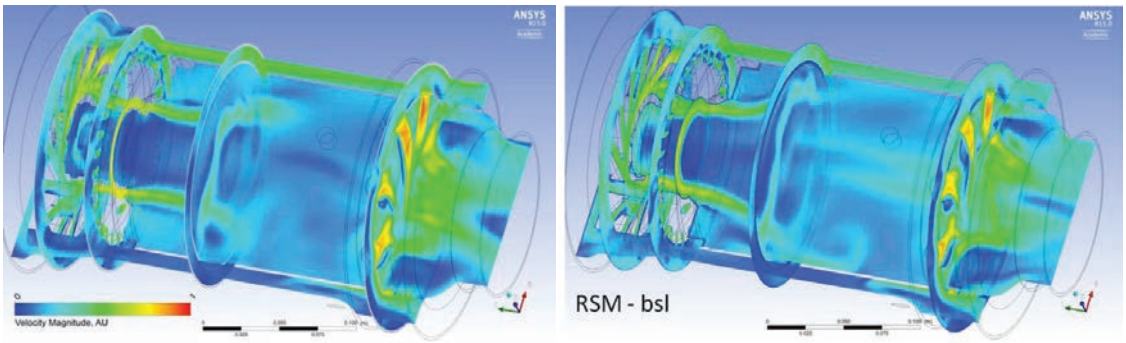

Fig. 4. Velocity profiles computed for GF (left) and LF (right) combustors by using RSM turbulence model

As expected, the main difference is in correspondence of the confluence of the flows from the first swirler to the inner zone of the combustor. Indeed, the geometry of the first swirler is different in GF and LF designs and, very relevant, there are no confinement walls in that zone for the LF one. As concerns the GF combustor, it is significant to note that the present results are in excellent agreements with previous studies on the Turbec T100 combustor when similar boundary conditions are adopted [14].

2.3. Definition of boundary conditions

In order to study the combustion process 3D CFD simulations were integrated by results of numerical studies based on matching analysis. A parametric thermodynamic analysis coupled with the adoption of operating maps of compressor and turbine published in literature [15] allows to individuate boundary and initial conditions in different operating points and for different liquid fuels. The computational code adopted was validated in different cases and

for several gas turbines [16]. In the present application, it was calibrated using experimental data taken in various ambient conditions, during operation of a Turbec T100 fed by natural gas.

Figure 5 shows the operating domain obtained in case of jet-A fuel, as reference fuel, at environmental conditions of 22°C and 1 bar. The parametric analysis was taken by varying rotational speed and fuel mass flow as a function of the shaft power expressed in kW. The domain is the locus of all possible operative conditions, for which there is a matching between compressor and turbine maps and the compliance with limits and closure conditions of the numerical model adopted. The MGT running line is shown with a tick black line.

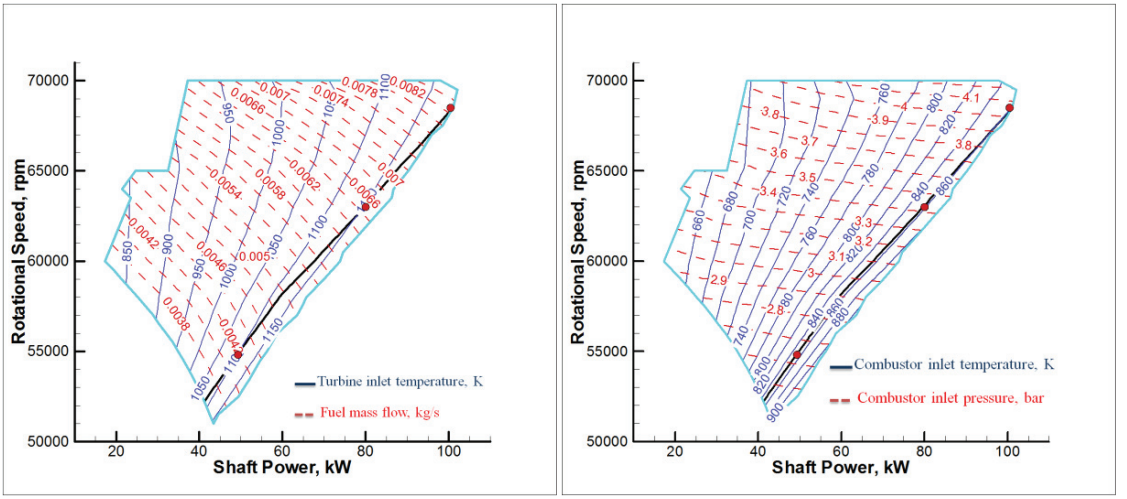

Fig. 5. Operating domain of MGT with in evidence variations of thermodynamic parameters with load

It is important to underline that the Turbec T100 control system requires to run at a fixed turbine outlet temperature of 918 K. In these conditions the risk of damaging turbine and heat exchanger is strongly reduced. In Figure 5 (a) turbine inlet temperature and fuel mass flow variations are reported; Figure 5 (b) presents two boundary conditions for CFD analysis: combustor inlet temperature and pressure. The combustor inlet temperature presented small variations along the running line, while the pressure decreases by decreasing the load. This behavior can be probably due to a coupled effect of the imposed TOT and the increasing of heat exchanger efficiency with load decreasing. It has to be underlined that another fundamental parameter that presents great variations with load is the air mass flow. The red circles in Figure 5 represent three different load conditions, at a shaft load of 100 kW, 80 kW and 50kW, that were simulated in the CFD computations. Table 5 reports the performance data and boundary conditions for the CFD simulations that will be discussed in the next section.

The efficiency takes into account of both thermal and mechanical efficiency but it does not consider the inverter efficiency and the power consumption related to auxiliaries.

Table 5. Results of matching analysis and boundary conditions for CFD simulations at different loads

Load	100%	80%	50%
Efficiency, -	0,28	0,29	0,25
Total Air Fuel Ratio, -	91	100	120
Air mass flow, kg/s	0.756	0.648	0.502
Fuel mass flow, kg/s	0.0083	0.00648	0.0042
Combustor inlet pressure, bar	4.06	3.42	2.65
Combustor inlet temperature, K	859	859	850

3. Results

3.1. Models adopted for liquid fuel CFD analysis

The adopted kinetic mechanisms are embedded in ANSYS CFX [8] and derived from Westbrook & Dryers [17].The injector was modelled defining a particle injection region just after the third swirl, as a cone with primary breakup. In particular a linearized Instability Sheet Atomization (LISA) model [8,18,19] was adopted for particles breakup. This is a valid model for pressure swirled atomization, typical of simulating gas turbine combustor injector. In absence of experimental data, nominal parameters were adopted to set the model.

The angle of the spray cone and injection pressure were fixed to 45° and 10 bar, respectively, according to the manufacturer specifications. The temperature of fuel was 300 K.

3.2. Part load behavior

Table 6 shows the differences mean value of turbine inlet temperature and concentrations of O_2 and CO_2 at the outlet of the combustor as predicted by the 0D and CFD numerical approaches.

Table 6. Results of CFD simulations

Load	100%	80%	50%
Turbine inlet Temperature, K (0D)	1178	1161	1099
Turbine inlet Temperature, K (CFD)	1180	1174	1156
[O2] at the combustor outlet, %	17.89	17.93	17.93
[CO2] at combustor outlet, %	1.89	1.86	1.79

0D and CFD simulations are in good agreement for 100% and 80% loads. Figures 6 and 7 report, for these two cases, velocity and temperature profiles in an axial surface and in six different cross section. The main difference regards the reduction with load of the zone at higher temperature, even if the mean value of temperature at the outlet differs less than 10 K.

It is evident that the greater difference between thermodynamic and CFD simulations concerns the 50% case. The turbine inlet temperature result of CFD analysis is greater than 50 K. Differently from the previous cases, at lower load the combustion process starts farther from nozzle and in a zone of the combustor close to the walls. In these conditions the combustor could be irreparably damaged and the temperature profile at the outlet could be strongly inhomogeneous with high temperature zones that could damage also the turbine blades. This aspect is also highlighted in Figure 9 that shows the oxidation molar reaction rate at different loads.

It is evident that with the hypothesis assumed for the atomization model, and consequently for the type of injector, the MGT presents critical operation conditions at partial loads.

Although the results of 0D matching analysis showed the possibility of adopting liquid fuels in a wide operating range, CFD simulations have underlined that the choice of the injector could be predominant respect to any modification of the combustion chamber geometry.

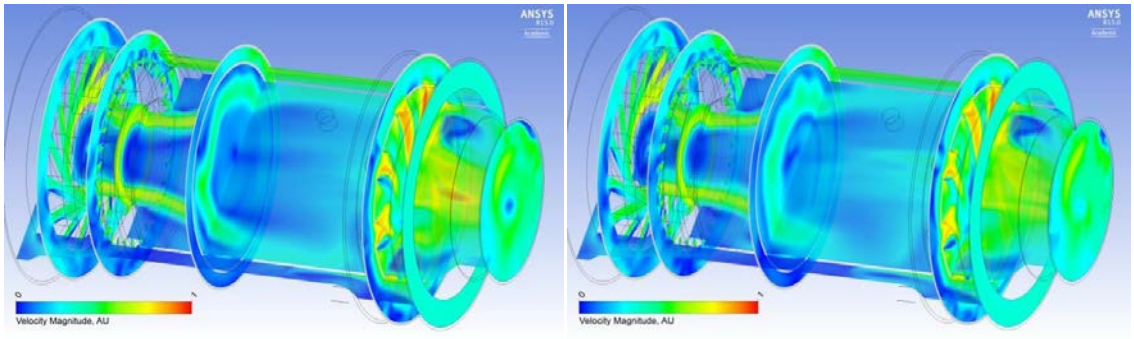

Fig. 6. Velocity distributions at (a) full load and (b) 80% load

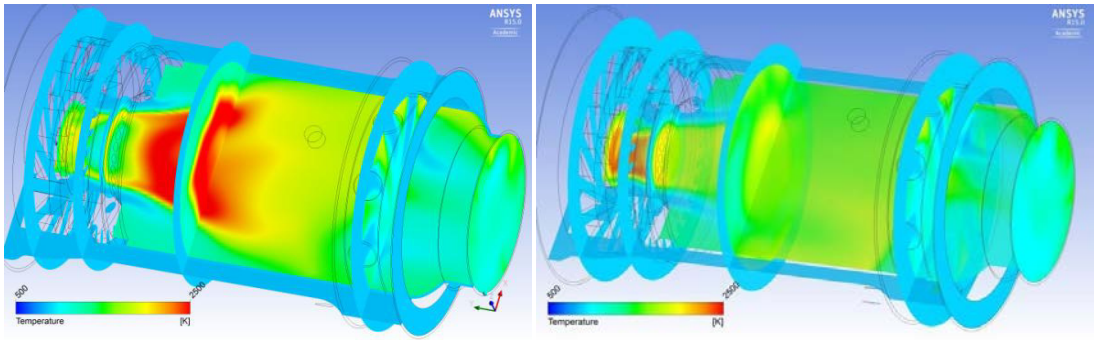

Fig. 7. Temperature profile at (a) full load and (b) 80% load.

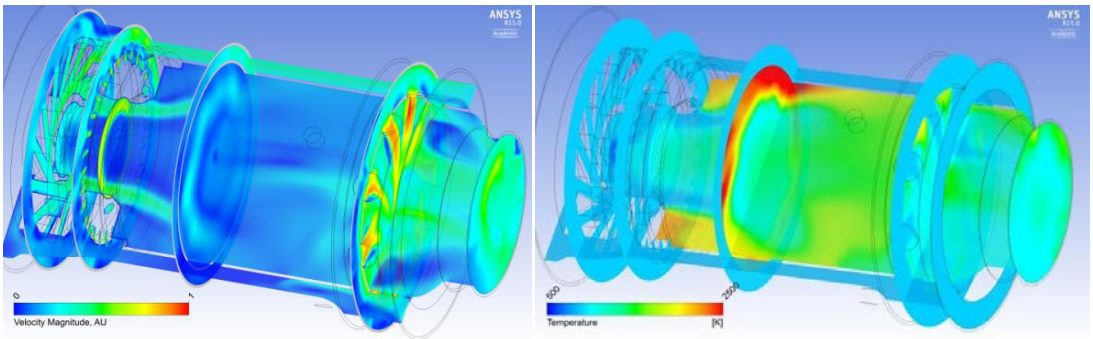

Fig. 8. Combustor behavior at 50% of load: (a) velocity profile; (b) temperature profile.

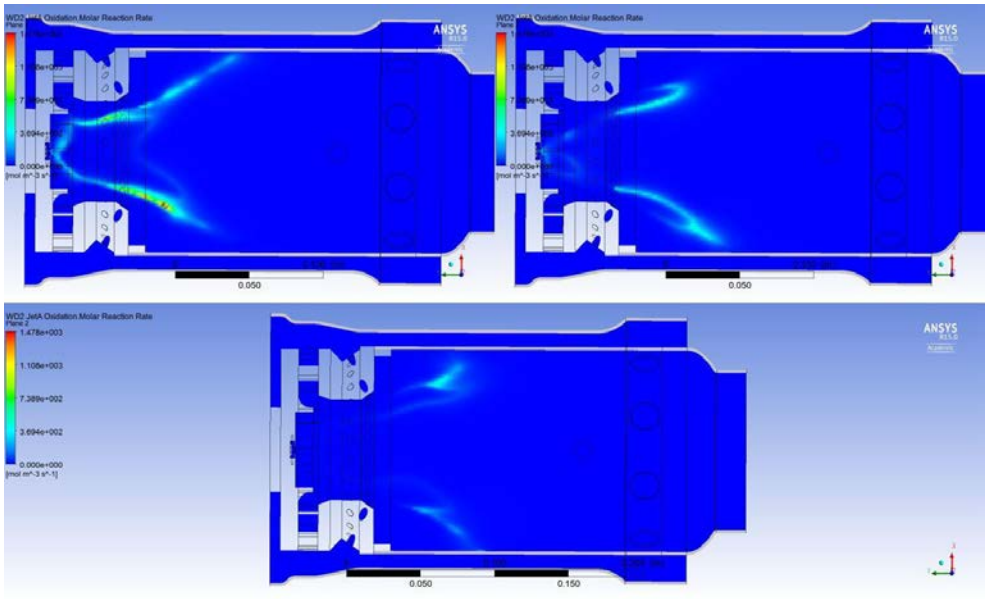

Fig. 9. Combustor behavior: jet-A oxidation molar reaction rate at (a) 100%; (b) 80% and (c) 50% load

In order to investigate the influence of the atomization on the combustion quality, additional simulations were done by varying the injection pressure from 10 to 15 bar. As shown in Figure 10, by increasing the injection pressure there is a better spray atomization in terms of droplet mean diameter ($\phi < 50$ μm), as highlighted by reduction of red zone, and an increasing of droplet velocity. The latter phenomenon is responsible of a lower residence time of the droplets in the primary combustion region which causes a worse evaporation: in fact it is evident droplets impact to liner walls.

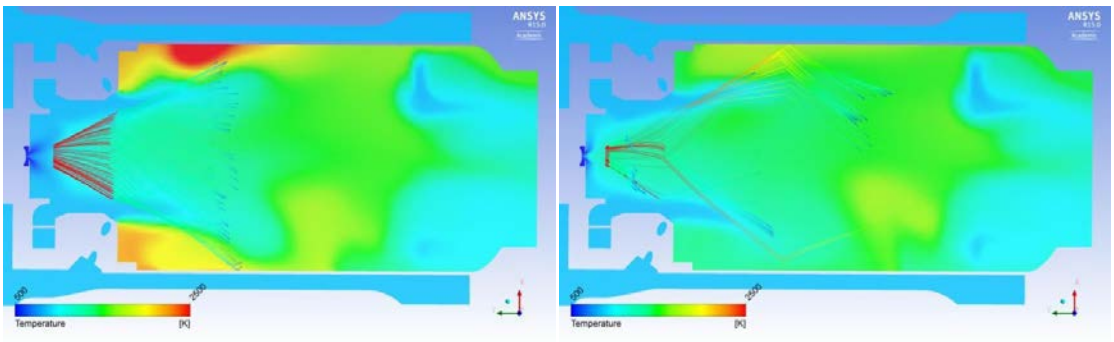

Fig. 10. Temperature profile and droplet tracking at 50% load for injection pressure of 10 bar (left) and 15 bar (right)

It was also analyzed the influence of the atomization angle. In Table 7 they are shown results of simulations for a half atomization angle of 12.5° and a injection pressure of 10 bar.

Table 7. Results of CFD simulations

Load	100%	80%	50%
Turbine inlet Temperature, K (0D)	1178	1161	1099
Turbine inlet Temperature, K (CFD)	1144	1120	1122
[O2] at the combustor outlet, %	18.12	18.26	18.4
[CO2] at combustor outlet, %	1.678	1.38	1.61

An injector with a reduced atomization angle seems to be eligible to work at 50% of load, as shown in figure 11. It should be underlined that the concentrations of CO2 and O2 showed in table 7 describe a worse combustion process respect the first case and also the turbine inlet temperature are lower, except for the case at 50% of load.

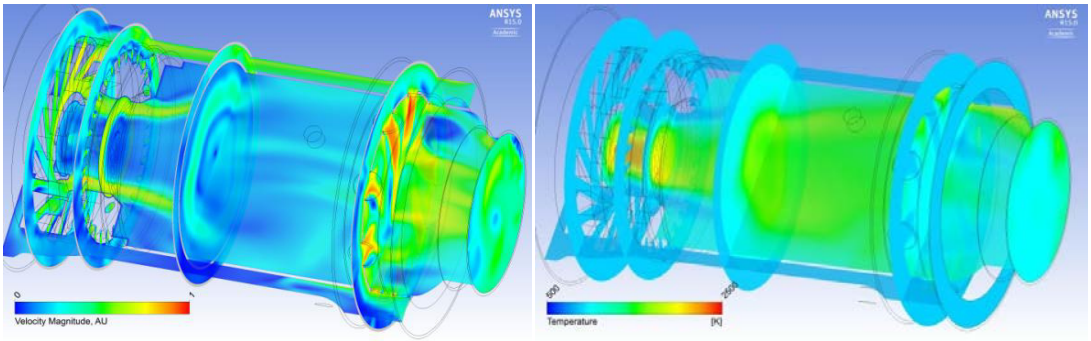

Fig. 11. Combustor behavior at 50% of load: (left) velocity and (right) temperature profile. Injector half cone of 12,5°;injection pressure P=10 bar.

A final consideration regards the injector location, in order to evaluate the effects of orientation and position of the single injector. Focusing only on the most critical case, load at 50%, two possible alternative solutions were evaluated: the effects of the inclination of the injector and the variations related to a different position of this. Figure 12 shows the temperature profiles and the droplet tracks, coloured according to the mean diameter of the droplets (red equal to 100 μm).

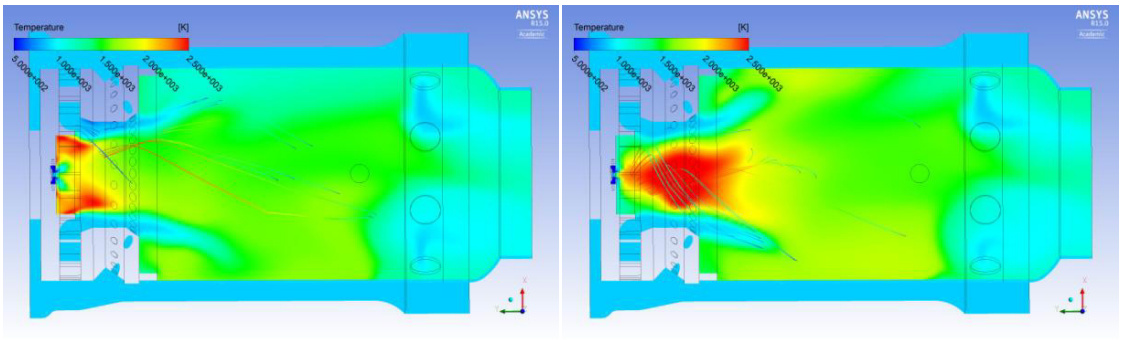

Fig. 12. Combustor behavior at 50% of load: (left) central injector inclined of 45°; (right) lateral injector inclined of 45°

In particular Figure 12 highlights that a different inclination could lead to a reduction of the ignition delay, the location of the injector assumes great importance. The left figure shows that in case of a central injector inclined of 45° respect the symmetry axis, the ignition delay is reduced and combustion occurs around the injector, while there

was a partly bad atomization. In case of a not centred injector, the coupled effect of inclined injection and swirled air mass flow allows a better atomization and a combustion confined in the inner zone of combustor, as requested. According to these preliminary results, positioning of the injector is critical in the optimization of the combustion quality.

4. Conclusions

The results of this preliminary numerical analysis offer several advices which can be useful to individuate potentialities and critical issues related to the behavior of a liquid fuelled Turbec T100.

Despite the limitations due to the lack of experimental data, the study highlights some of the main aspects to be addressed. Even if the results of a 0D thermodynamic analysis of matching indicated that the operating domain of the MGT was wide and that the traditional running line of the Turbec T100 (TOT = 918 K) crossed all the power range, the CFD analysis of the combustor highlighted several critical issues, in particular at part load conditions. Once fixed the geometry of the combustion chamber, which is slightly different respect the commercial model designed for natural gas feeding, an efficient combustion process depends also on the injector design. In particular the choice of the type of injector, in terms of injection pressure, atomization angle and position, must take into account the high variability of the boundary conditions at varying loads. In particular, a central single pressure swirled atomizer operating at fixed injection pressure seems to provide an efficient combustion process just at full load but various critical issues rose at part load conditions. The influence of single injection parameters was also examined, focusing in particular on the position of the injector. Further studies are required to establish the optimal position and characteristics of the fuel injection system.

Acknowledgements

The research was partially supported by the Italian Ministry of Economic Development within the framework of the Program Agreement MiSE-CNR “Ricerca di Sistema Elettrico”.

References

[1] Decision No 406/2009/EC of the European Parliament and of the Council, Official Journal of the European Union, L 140/136, 5.6.2009.
[2] Chiaramonti D., Rizzo A.M., Spadi A., Prussi M. , Riccio G., Martelli F., Exhaust emissions from liquid fuel micro gas turbine fed with diesel oil, biodiesel and vegetable oil, Applied Energy, 2013; 101:349-356
[3] Chiariello F., Allouis C., Reale F., Massoli P., Gaseous and particulate emissions of a micro gas turbine fuelled by straight vegetable oil-kerosene blends, Exp. Therm. Fluid Sci., 2014; http://dx.doi.org/10.1016/j.expthermflusci.2013.11.013
[4] Reale F.,Calabria R., Chiariello F., Massoli P., Pagliara R., Piazzesi R., Numerical and experimental study of a micro gas turbine combustor, Proceedings of Turbulence, Heat and Mass Transfer 7, 2012); doi: 10.1615/ICHMT.2012.ProcSevIntSympTurbHeatTransfPal.1590
[5] Calabria R., Chiariello F., Massoli P.. M Reale F. , Part load behavior of a micro gas turbine fed with different fuels, ASME paper GT2014-26671, 2014
[6] Reale F., Calabria R., Chiariello F., Pagliara R., Massoli P., A micro gas turbine fuelled by methane-hydrogen blends, Applied Mechanics and Materials, 2012; 232, 792
[7] Chiariello F., Reale F., Calabria R., Massoli P., Off design behavior of a 100kW Turbec T100P micro gas turbine, Applied Mechanics and Materials, 2013; 390 , pp. 275-280
[8] Ansys CFX Theory Guide
[9] Durbin P.A., Pettersen Reif B.A.: Statistical theory and modeling for turbulent flows, John Wiley and Sons Ltd 2003.
[10] Wilcox D. C.: Turbulence Modeling for CFD, DCW Industries Inc., 2. Edition, 1998.
[11] Rodi W. :Turbulence models and their application in hydraulics. Taylor and Francis, 1993
[12] Launder B.E., Spalding D.B.: Lectures in mathematical models of turbulence. Academic Press, 1972
[13] Menter, F.R.: Two-equation eddy-viscosity turbulence models for engineering applications, AIAA Journal, 1994; Vol. 32, No. 8, pp. 1598-1605.
[14] Hohloch M., Zander J., Widenhorn A., Aigner M. Experimental characterization of a micro gas turbine test rig, ASME paper no. GT2010-22799, 2010
[15] Caresana F., Pelagalli L., Comodi G., Renzi M., Microturbogas cogeneration systems for distributed generation: Effects of ambient temperature on global performance and component's behavior, Applied Energy, 2014; n. 124, p. 17–27.
[16] Bozza F., Cameretti M.C., Tuccillo R., “Adapting the micro-gas turbine operation to variable thermal and electrical requirements”, ASME Paper 2003-GT-38652, 2003

[17] Westbrook K., Dryer F. L., Simplified reaction mechanisms for the oxidation of hydrocarbon fuels in flames", Combustion Science and Technology, 1981; Vol. 27, pp. 31-43
[18] Schmidt D. P., Nouar I., Senecal P. K., Rutland C. J., Martin J. K., Reitz. R. D. Pressure-swirl atomization in the near field. SAE Paper 01-0496. SAE, 1999.
[19] Senecal, P.K., Schmidt, D.P., Nouar, I., Rutland, C.J., Reitz, R.D., Corradin, M.L., modeling high-speed viscous liquid sheet atomization", International Journal of Multiphase Flow,1999; 25, pp. 1073-1097.